International Journal of New Horizons in Physics

http://dx.doi.org/10.18576/ijnhp/030105

The Effect of Cu Substitution on Structural, Magnetic and Catalytic Properties of $ZnFe_2O_4$ Synthesized by Microwave Combustion Method

M. H. Mahmoud [1,*], *Azza M. Hassan* [1] *and Abd El-Aziz A. Said* [2]

[1] Physics Department, Faculty of Science, Assiut University, Assiut 71516, Egypt.
[2] Chemistry Department, Faculty of Science, Assiut University, Assiut 71516, Egypt.

Received: 21 Sep. 2015, Revised: 22 Dec. 2015, Accepted: 24 Dec. 2015.
Published online: 1 Jan. 2016.

Abstract: Nanocrystalline Zn1-xCuxFe2O4 ferrites with x = 0.0, 0.05, 0.10, 0.15, 0.20, 0.25 and 0.50 were prepared by microwave assisted combustion method using metal nitrates and glycine as a fuel. Structural properties of the as-synthesized powders were characterized by X-ray diffraction patterns (XRD). The magnetic properties were measured using vibrating sample magnetometer (VSM). XRD analysis indicates the prepared samples are highly crystalline and they have fine structure, where their crystallite sizes are in the nanoscale range from 20-40 nm. The Saturation magnetization (Ms) and magnetic moment show an increase with Cu content (x) up to x = 0.2 reached to about 58 emu/g, and then it decreases slightly. The catalytic performance for the as prepared samples was carried out using dehydration-dehydrogenation of isopropanol. The results revealed that the catalytic conversion of isopropanol increases with Cu substitution. The isopropanol conversion reached to about 99% with 76% and 24% yields of acetone and propene respectively.

Keywords: Cu-Zn ferrite; Microwave combustion method; Nanoparticles; Magnetic properties; Catalyst.

1 Introduction

The substituted spinel ferrites have attracted attention due to their technological applications such as electronic, magnetic and microwave devices [1-6]. Their properties depend mainly on the concentration; type of substituted metal ions and their distribution over tetrahedral and octahedral sites [7-9]. Cu-substituted ferrites are promising materials in applications. Introducing copper into ferrites with spinel structure causes appreciable changes in their properties, particularly structural ones, as it would possibly create a lattice distortion due to Jahn-Teller effect, dielectric, and magnetic properties. Also the catalytic performance of the ferrite is enhanced with Cu substitution, due to the different redox properties of Cu [10, 11].

Recent investigations of spinel ferrites indicated that Zinc ferrites in the nanoscale show anomalous magnetic properties [12]. There are many studies of the electrical, optical and magnetic properties of Cu- substituted Zn ferrites [13-16]. These studies revealed that the magnetic properties are enhanced, the band gap energy decreases, and high dielectric constant is observed with increasing Cu content.

It is well known that synthesis method has an effective role on the structural and magnetic properties of ferrites. Spinel ferrite nanoparticles have been prepared by several methods such as microemulsion method [17], ball milling [18], and the sol–gel method [19]. Recently Microwave assisted combustion method has attracted the interest of synthesis nano ferrites as a simple, fast and low cost process [20-21]

The present work aims to investigate the magnetic properties of nanocrystalline Zn1-xCuxFe2O4 ferrites with x = 0.0, 0.05, 0.10, 0.15, 0.20, 0.25 and 0.50 prepared successfully by microwave assisted combustion method using glycine as a fuel. The catalytic activity of the prepared samples was tested using dehydrogenation – dehydration of isopropanol over the samples.

2 Experimental

2.1 Materials and methods

$Zn_{1-x}Cu_xFe_2O_4$ nanoparticles (x = 0.00, 0.05, 0.10, 0.15, 0.2, 0.25, and 0.50) were prepared from an exothermic reaction of a mixture of metallic nitrates (Zn, Cu and Fe) and glycine (reducing agent) at glycine: metal nitrate ratio equal to 0.5:1. A stoichiometric ratios of zinc nitrate ($Zn(NO_3)_2.6H_2O$), Copper nitrate ($Cu(NO_3)_2.3H_2O$), ferric nitrate ($Fe(NO_3)_3.9H_2O$), and an appropriate amount of glycine (NH_2CH_2COOH) were dissolved in a minimum quantity of water (see table 2.1). The crucible containing the solution

*Corresponding author e-mail: mohom63@yahoo.com

was introduced into a microwave-oven at a maximum power of 800W for several minutes. The solid powder was obtained after around 20 min.

2.2 Characterizations and measurements

Phase identification of the samples was performed using X-ray diffractometer equipped with an automatic divergent slit (XRD; Philips PW1700 diffractometer, Netherlands). Diffraction patterns were obtained using CuKα radiation (λ= 0.15418 nm) and a graphite monochromator in the 2θ range from15° to 70°. The patterns were fitted using pseudo Lorentzian line shapes to account for the asymmetry of the peaks, and for accurate determination of lattice parameters and apparent crystallite size. The magnetic measurements were carried out at room temperature using vibrating sample magnetometer (VSM) Lakeshore Model 7410 equipped with 2T magnet. The specific surface areas of the catalyst samples were determined from Nitrogen adsorption-desorption isotherms, which measured at -196ºC using Quantachrome Instrument Corporation, USA (Model Nova 3200). Test samples were thoroughly out gassed for 2h at 150ºC to a residual pressure of 10^{-4} torr and the weight of the out gassed sample was that used in calculations.

The porosity of the catalysts determined from the desorption curve using Nova enhanced data reduction software (Version 2.13). The specific surface area of these nanoparticles was calculated by the BET equation. The catalytic activities of the samples were tested by the dehydration - dehydrogenation of isopropyl alcohol (IPA) at 250 ºC in a conventional fixed bed flow type Pyrex glass tube reactor at atmospheric pressure. A 0.5 g catalyst was placed in the middle of the reactor tube with quartz wool. In all tests, N_2 gas was used as carrier with a total flow rate of 50 ml min^{-1}. The temperature of the isopropanol in the saturator was set at 0ºC using dry ice. The reaction temperature was controlled with a Gallenkamp temperature controller. The exit feed was analyzed by direct sampling of the gaseous products into a Unicom PROGC gas Chromatograph using a flame ionization detector (FID). A mixture of IPA and N_2 was introduced into the reactor after nitrogen was bubbled through IPA saturator. The total flow rate was fixed at 50 ml min^{-1}. The gases after reaction were chromatographically analyzed by FID with a Unicam PROGC using a 10% PEG 400 glass column (2 m) for analysis of the reaction products of IPA on the tested catalysts. Measurement of the conversion and yield (%) were recorded after 1 h from the initial introduction of the reactant into the reactor to ensure the attainment of the reaction equilibrium, (steady state conditions).

3 Results and discussions

3.1 XRD analysis

In order to investigate the crystal structure of the obtained powder material, XRD analysis was performed and the resultant pattern of the prepared $Zn_{1-x}Cu_xFe_2O_4$ nanoparticles (x = 0.0, 0.05, 0.10, 0.15, 0.20, 0.25 and 0.50) are presented at Figures 1 and 2. It is noticed that all the prepared samples show good crystallinity. The broad peaks in the XRD patterns indicate a fine nature of the particles. Analysis of the diffraction patterns of the samples with

Table 1 Structural parameters of $Zn_{1-x}Cu_xFe_2O_4$ samples

Copper content (x)	crystallite size D (nm)	Lattice constant a_o(nm)
0.00	25.3	0.8410
0.05	32.8	0.8398
0.10	32.9	0.8404
0.15	32.3	0.8405
0.20	34.4	0.8402
0.25	28.8	0.8408
0.50	41.9	08408

$x \leq 0.2$ confirmed the formation of single phase spinel structure with no extra peaks corresponding to any other phases. However the sample with $x = 0.25$ shows additional small peaks characteristic of ZnO and CuO phases. The intensity of these impurity phases increases for the sample with x = 0.5. The formation of CuO phase with increasing the Cu concentration (x) was also observed in previous studies [22].

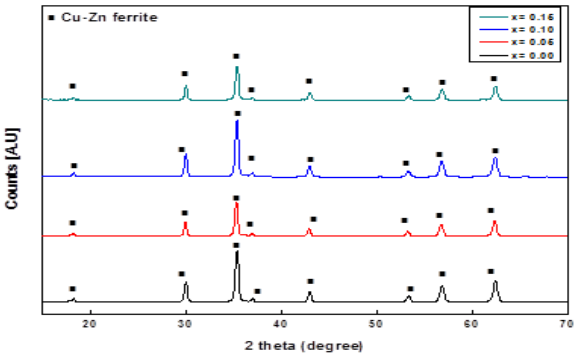

Figure 1 XRD patterns of the nanocrystalline $Zn_{1-x}Cu_xFe_2O_4$ samples ($x \leq 0.15$).

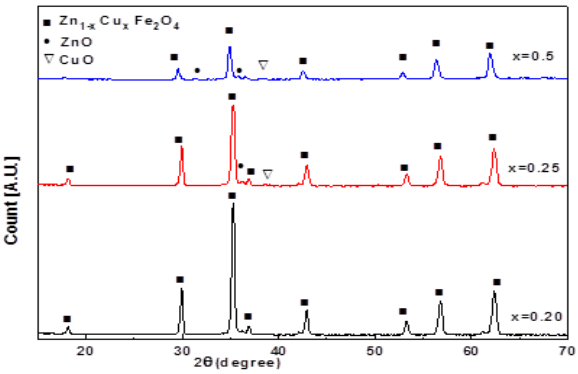

Figure 2 XRD patterns of the nanocrystalline $Zn_{1-x}Cu_xFe_2O_4$ samples (x= 0.20, 0.25 and 0.50).

The crystallite sizes of the prepared samples were calculated

using the Debye–Scherrer equation [23]. The lattice parameters for different compositions have been calculated using the values of d-spacing. Using the least square fit method [24], exact lattice constants a_0 was calculated. The obtained crystallite sizes and lattice constants values are given in Table 1. The average crystallite sizes are in the range of 20-40 nm for all compositions.

3.2 Magnetization studies

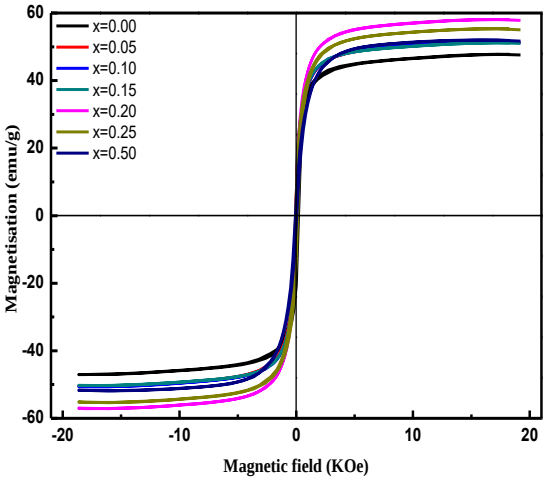

Figure 3 Room temperature M–H loops of the nanocrystalline $Zn_{1-x}Cu_xFe_2O_4$.

Table 2 Magnetic parameters of $Zn_{1-x}Cu_xFe_2O_4$ nanoparticles

Copper Content (x)	Hc (Oe)	Ms (emu/g)	Mr (emu/g)
0.00	45.9	47.4	5.3
0.05	67.3	51.0	7.0
0.10	50.5	51.0	5.9
0.15	42.9	50.0	5.2
0.20	65.6	57.6	7.6
0.25	65.6	55.3	6.6
0.50	83.2	51.9	5.1

To clarify the magnetic properties for $Zn_{1-x}Cu_xFe_2O_4$ nanoparticles, the room temperature magnetization measurements were performed on a vibrating sample magnetometer (VSM). The applied magnetic field is in the range from -20 to +20 kOe. The resultant M–H curves are shown in Figure 3. All The obtained M-H curves are saturated with hysteretic behaviours of soft ferrimagnetic materials.

The obtained magnetic parameters are listed in Table 2. From this table we notice that the as synthesized zinc ferrite sample has high magnetic parameters compared to bulk zinc ferrite [25-27].This indicates that nano scale zinc ferrite has partial inversion structure. The saturation magnetization increases with Cu^{2+} ions substituted up to $x = 0.2$, due to magnetic substitution of Cu ions ($1\mu_B$) compared to nonmagnetic Zn^{2+} ions ($0\ \mu_B$). It is well known that Cu^{2+} ions prefer occupying octahedral site [28-30]. So that Cu ions replace Zn ions in octahedral sites, and consequently the net magnetic moment increases. It is noticed that with more increasing of Cu amount at $x = 0.25\ and\ 0.5$ the saturation magnetization decreases slightly. This could be related to the presence of some of Cu^{2+} cations in tetrahedral sites which results in changing the strength of the superexchange interactions. As a result, the net magnetic moments decrease. Also we can suggest that Cu^{2+} replace some of Fe^{3+} ions which occupy octahedral sites leading to reduction of the net magnetic moment. As indicated by XRD in these samples, the appearance of small impurity phases may be another reason to decrease their magnetizations. The coercive field H_c was found to increase with Cu substitution reaching to a maximum value of about 83 Oe at x=0.50. This behaviour of coercive field could be attributed to anisotropy energy change as a result of Jahn-Teller effect.

As the copper amount increases in the spinel zinc ferrite, the spinel structure is distorted from cubic to tetragonal, due to the cooperative Jahn-Teller effect involved by the octahedrally coordinated Cu^{2+} ions [31].

3.3 Catalytic activity

The catalytic performance of $Zn_{1-x}Cu_xFe_2O_4$ nanoparticles was tested using IPA decomposition at reaction temperature equal to 250ºC. The results of catalytic evaluations are given in Table 3. From this Table we observe that the total conversion of IPA increases with increasing Cu substitution to reach to 99 % at $x = 0.50$ However; the catalytic activity of spinel ferrites is correlated mainly to the octahedral cations; it is well known that Cu^{2+} ions prefer octahedral occupation [32, 33]. So that increasing the concentration of the copper ions in the spinel structure facilitates the catalytic process. The obtained results revealed that IPA was converted into both acetone and propene over the samples, which suggested the presence of both acidic and basic sites on the surface of all samples. Acetone selectivity is higher than that for propene. This can be also correlated to the presence of more basic active sites than acidic sites in the samples.

As the Cu concentration increases the selectivity towards acetone formation increases due to an effective increase in the number of active sites contributing in dehydrogenation of IPA. On the other hand the selectivity towards propene formation decreases with Cu substitution which suggests a decrease in the number of active sites responsible for dehydration. This observation revealed that adding copper enhances generation of basic sites.

We can notice from Tables 2 and 3 that with increasing Cu substitution the magnetic properties and catalytic activity are enhanced. The catalytic activity of spinel ferrites are correlated to magnetization [34]. Also, the good catalytic performance of the prepared samples is not related to the measured specific surface area which is $S_{BET} \leq 3\ m^2/g$ of catalysts. This behaviour of specific surface area was observed previously [35, 36].

Table 3 Catalytic evaluations of $Zn_{1-x}Cu_xFe_2O_4$ samples.

Copper content X	Conversion %	Selectivity %		Yield %	
		Propene	Acetone	propene	Acetone
0.00	47	45.8	54.2	21.5	25.5
0.05	59.5	25.2	74.8	15.0	44.5
0.10	98.0	26.8	73.2	26.3	71.7
0.15	99.0	24.6	75.4	24.3	74.6
0.20	99.0	22.4	77.6	21.5	74.3
0.25	99.0	22.5	77.5	22.2	76.7
0.50	99.0	22.8	77.2	22.6	76.4

4 Conclusion

The $Zn_{1-x}Cu_xFe_2O_4$ nanoparticles were successfully synthesized by microwave assisted combustion method. The XRD investigation confirmed the formation of a single – phase of cubic spinel ferrites of the samples with $x \leq 0.2$, However; the samples of x= 0.25 and 0.5 show additional small peaks characteristic of ZnO and CuO phases. The magnetic properties of the samples were investigated by VSM. The results indicate augmentation the saturation magnetization with increasing x up to 0.2 and then slightly decrease. The investigated samples are active in the reaction of catalytic isopropanol decomposition. The results indicate that their catalytic activity increases with Cu substitution. Also the selectivity toward acetone increases with increasing x, while propene selectivity decreases.

References

[1] R. Wu, J. Qu, H. He, Y. Yu, Applied Catalysis B: Environmental 48 (2004) 49–56.

[2] J. Sláma, M. Šoka , A. Grusková , R. Dosoudil, V. Jancárik, Jarmila Degmová, Journal of Magnetism and Magnetic Materials 326 (2013) 251–256.

[3] J. Sláma, A.Grusková, M. Ušáková, E. Ušák, R. Dosoudil, Journal of Magnetism and Magnetic Materials 321 (2009) 3346–3351,

[4] Y.P. Fu, C.H. Lin, Journal of Magnetism and Magnetic Materials 251 (2002) 74–79.

[5] K. Praveena, K. Sadhana, S.R. Murthy, Materials Research Bulletin 47 (2012) 1096–1103.

[6] R.V. Mangalaraja , S. Ananthakumar, P. Manohar, F.D. Gnanam, Materials Letters 57 (2003) 1151– 1155.

[7] T.J. Shinde, A.B. Gadkari, P.N. Vasambekar, Journal of Magnetism and Magnetic Materials 333 (2013) 152–155.

[8] S. Verma, P.A. Joy, S. Kurian, Journal of Alloys and Compounds 509 (2011) 8999–9004.

[9] A. R. Lamani, H.S. Jayanna, P. Parameswara, R. Somashekar, Ramachander, R. Rao, G.D. Prasanna, Journal of Alloys and Compounds 509 (2011) 5692–5695.

[10] M. Banerjee, N. Verma, R. Prasad, J Mater Sci (2007) 42:1833–1837.

[11] A. S. Albuquerque, M.V.C. Tolentino, J. D. Ardisson, F.C.C. Moura, R. Mendonc, W.A.A. Macedo, Ceramics International 38 (2012) 2225–2231.

[12] M. G. Naseri, E. B. Saion, M. Hashim, A. H.Shaari, H. A. Ahangar, Solid State Communications 151 (2011) 1031–1035.

[13] A. Manikandan, J. Judith Vijaya, L. John Kennedy, M. Bououdina, Journal of Molecular Structure 1035 (2013) 332–340.

[14] O. Mounkachi, M. Hamedoun, M. Belaiche, A. Benyoussef, M. Sajieddine, Solid State Communications 151 (2011) 938–942.

[15] M.U. Rana, T. Abbas, Journal of Magnetism and Magnetic Materials 246 (2002) 110-114.

[16] A. Maqsood, M. Ajmal, Journal of Alloys and Compounds 460 (2008) 54–59.

[17] Y. Ahn, E.J. Choi, S. Kim, H.N.Ok, Materials Letters 50 (2001) 47–52.

[18] T. Verdier, V. Nachbaur, M. Jean, Journal of Solid State Chemistry 178 (2005) 3243–3250.

[19] Z. Klencsár, Gy. Tolnai, L. Korecz, I.Sajó, P. Németh, J. Osán, S. Mészáros,E. Kuzmann, Solid State Sciences 24 (2013) 90-100.

[20] V. Vasanthi, A. Shanmugavani, C. Sanjeeviraja, R. Kalai Selvan, Journal of Magnetism and Magnetic Materials 324 (2012) 2100–2107.

[21] Y.-P. Fu, K.-Y. Pan, C.-H. Lin, Materials Letters 57 (2002) 291– 296

[22] M.H. Mahmoud, A.M. Elshahawy , S. A. Makhlouf, H.H. Hamdeh, Journal of Magnetism and Magnetic Materials 343 (2013) 21–26.

[23] N.F.M. Henry, J. Lipson and W.A. Wooster, The Interpretation of X-Ray Diffraction Photographs (Macmillan and Co Ltd., London, 1951).

[24] M. Sertkol, Y. Köseoglu, A. Baykal, H.Kavas, A. Bozkurt, M.S. Toprak, Journal of Alloys and Compounds 486 (2009) 325–329.

[25] N. M. Deraz and A. Alarifi,Int. J. Electrochem. Sci., 7 (2012) 3798 – 3808.

[26] E. J. Choi, Y.k. Ahn, E. J.Hahn, Journal of the Korean Physical Society, Vol. 53, No. 4, October 2008, 2090-2094.

[27] A. Pradeep, P. Priyadharsini, G. Chandrasekaran, Journal of Alloys and Compounds 509 (2011) 3917–3923

[28] S.S. Ata-Allah, A. Hashhash, Journal of Magnetism and Magnetic Materials 307 (2006) 191–197.

[29] M.A. Gabal, Y.M. Al Angari, M.W. Kadi, Polyhedron 30

(2011) 1185.

[30] J. Balavijayalakshmi, N. Suriyanarayanan, R. Jayapraksah, Mater. Lett. 81(2012) 52.

[31] C. Villette, F. Agnoli, Ch. Bonino, Ph. Tailhades, A. Rousset, Magnetic Hysteresis in Novel Magnetic Materials Ch 10, (1997) 389-393.

[32] A.S. Albuquerque, M.V.C. Tolentino, J.D. Ardisson, F.C.C. Moura, R. Mendonc, W.A.A. Macedo, Ceramics International 38 (2012) 2225–2231.

[33] E. Manova, T. Tsoncheva, D. Paneva, M. Popova, N. Velinov, B. Kunev, K. Tenchev, I. Mitov, Journal of Solid State Chemistry 184 (2011) 1153–1158.

[34] J.A. Toledo-Antonio, N.Nava, M. Martínez, X. Bokhimi, Applied Catalysis A: General 234 (2002) 137–144.

[35] M. Kooti, A. Naghdi Sedeh, Scientia Iranica, (2012).

[36] G. N. Pirogova, N. M. Panich, R. L Korosteleva, Yu.V. Voronin, G. E. Kalinina, Russian Chemical Bulletin, 45(1) (1996) 42– 44.